Advances in Reliability, Safety and Security, Part 4 – Kołowrocki, Dąbrowska (eds.)
 ISBN 978-83-68136-16-6 (printed), ISBN 978-83-68136-03-6 (electronic)

Advances in Reliability, Safety and Security

ESREL 2024
Monograph Book Series

Bayesian Regularized Artificial Neural Network For Estimating Ignition Probability In Oil And Gas Plants

Stefano Marchetti[a], Francesco Di Maio[a], Enrico Zio[b,a], Luca Decarli[c], Laura La Rosa[c], Giuseppe Nicotra[c], Andrea Tortora[c], Anna Crivellari[c], Salvatore Cincotta[c]

[a]*Energy Department, Politecnico di Milano, Milano 20156, Italy.*
[b]*MINES Paris-PSL, Centre de Recherche sur les Risques et les Crises (CRC), Sophia Antipolis, France.*
[c]*Eni Natural Resources – HSEQ, via Emilia 1, 20097 San Donato Milanese, Italy.*

Abstract

In the Quantitative Risk Assessment (QRA) of Oil & Gas (O&G) plants, the Ignition Probability (IP) following a release of flammable gaseous material can be estimated by the MISOF (Modelling of Ignition Sources on Offshore oil and gas Facilities) model, that requires time-consuming simulations (e.g., by Computational Fluid Dynamic (CFD)) for calculating the flammable volume released. By this way, only a limited number of accidental scenarios can be considered, which may lead to inaccurate IP estimates. To overcome this limitation, in this work a Bayesian Regularized Artificial Neural Network (BRANN) is proposed together with a pre-processing of the input data to match the training data. This enables the BRANN to provide accurate IP estimates. The results obtained in the case of a separator unit of a real O&G plant demonstrate the applicability of the BRANN, its ability to outperform conventional piecewise polynomial regression with a reduced number of CFD simulations.

Keywords: Quantitative Risk Assessment (QRA), Ignition Probability (IP), Computational Fluid Dynamic (CFD), Bayesian Regularized Artificial Neural Network (BRANN)

1. Introduction

The escalation of fires following a Loss Of Primary Containment (LOPC) is one of the main concerns in the Oil & Gas (O&G) industry (ISO 17776, 2016). Estimating the Ignition Probability (IP) following the release of flammable gaseous material is necessary for the Quantitative Risk Assessment (QRA) of O&G plants and can be done, using the MISOF (Modelling of Ignition Sources on Offshore oil and gas Facilities) model (MISOF, 2018; Cincotta et al., 2021). Computational Fluid Dynamic (CFD) simulation is used to calculate the time-dependent flammable volume released, to be provided in input to the MISOF model (Agranat et al., 2007; Zhang and Chen, 2010). CFD simulations are time demanding and considering a limited number of accidental scenarios can possibly lead to inaccurate IP estimates (Jin and Jang, 2018; Vianna and Cant, 2012). To overcome this limitation, a Bayesian Regularized Artificial Neural Network (BRANN) has been proposed in (Di Maio et al., 2021a). The BRANN can be trained with a limited number of CFD simulations available and once trained it can be used in accidental scenarios with input values (e.g., release source, ignition source, confinement level, congestion level, wind strength, gas mixture, LOPC hole size and number of detectors) similar to those of the training dataset. This may not be the need in practice, in particular for the LOPC hole sizes to consider for the IP calculation. In this work, we develop a preprocessing strategy for calculating an equivalent of a generic LOPC hole size to match one available in the training dataset, so as to allow using the BRANN also for input values different from those of the training dataset.

The proposed method is applied to one of the separator functional units of a real O&G plant trained with a limited dataset of input-output patterns. The results demonstrate the enhanced applicability of the BRANN enabled by the preprocessing strategy that calculates the equivalent LOPC hole.

The paper is organized as follows: Section 2 recalls the MISOF model, Section 3 presents the regression model approach typically used, Section 4 describes the novel BRANN, Section 5 shows the results of its application to the case study and in Section 6 conclusions are drawn.

2. The MISOF ignition model

In general terms, the IP hereafter symbolically indicates as $P(I)$ is defined as the product of the probability of exposure $P(E)$ of a live ignition source to a flammable atmosphere and the probability of ignition given such exposure $P(I|E)$ (MISOF, 2018):

$$P(I) = P(E) \cdot P(I|E) \tag{1}$$

In this work, for simplicity and without loss of generality, we conservatively assume that $P(E) = 1$, so that $P(I) = P(I|E)$.

The MISOF approach is used to evaluate $P(I|E)$, accounting for both "immediate" ignition and "delayed" ignition mechanisms (IOGP 434-06, 2019), Figure 1.

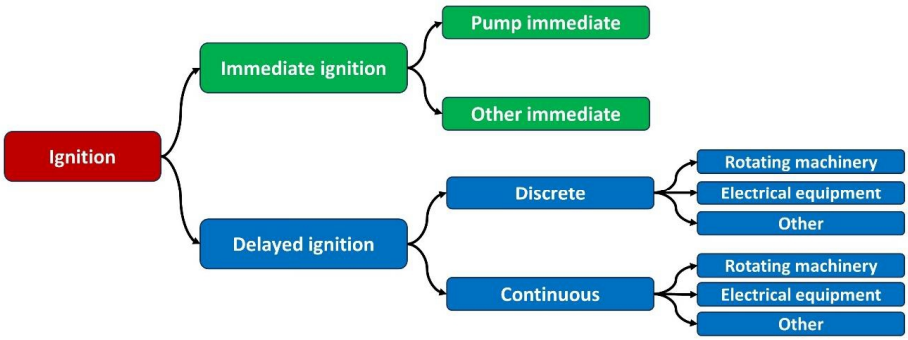

Fig. 1. P(I|E) contributions according to MISOF model.

2.1. Immediate ignition

Immediate ignition mechanisms are those occurring immediately after the LOPC, before the flammable cloud is formed, and can cause Jet Fires (JFs) or Pool Fires (PFs), depending on the pressure of the system. The immediate IP, $P_I(I)$, is evaluated accounting for two main contributions (MISOF, 2018), whose values considered in this work are listed in Table 1:

- pump immediate ignition contribution, accounting for ignition caused by leaking pumps;
- other immediate ignition contributions, accounting for ignition caused by any other equipment.

Table 1. $P_I(I)$ of different contributions.

Immediate ignition source	$P_I(I)$
Pumps	0.072
Other	0.0007

2.2. Delayed ignition

Delayed ignition mechanisms are those occurring after the formation of a flammable cloud following the LOPC and can cause Flash Fires (FFs) or Explosions (EXs), depending on the congestion level of the area. Typically, the time-dependent behavior of the flammable cloud is discretized into N time steps, each of duration Δt, and two different types of delayed ignition mechanisms are considered: continuous and discrete. Continuous ignition sources are those that are always present (e.g., a flame or a hot surface) and ignite the flammable cloud at the moment of the exposure. Discrete ignition mechanisms are those that are effective only at distinct instants (e.g., portable "Non-Ex" equipment). Both mechanisms can be caused by rotating machinery (such as pumps and compressors), electrical components (such as high voltage instruments) and others (including any source which is not rotating machinery nor electrical equipment). The continuous delayed IP $P_C(t_i)$ and the discrete delayed IP $P_D(t_i)$ at the ***i-th*** time step t_i are calculated as follows (MISOF, 2018):

$$P_C(t_i) = 1 - e^{-\lambda_C \cdot V_{new}(t_i) \cdot F_C(t_i)} \tag{2}$$

$$P_D(t_i) = 1 - e^{-\lambda_D \cdot V_D(t_i) \cdot \Delta t \cdot F_D(t_i)} \tag{3}$$

where λ_C is the expected number of ignitions per m^3 of flammable volume due to continuous ignition mechanisms, λ_D is the expected number of ignitions per m^3·s due to discrete ignition mechanisms, $V_{new}(t_i)$ is the new volume of flammable material exposed to the flammable cloud during the ***i-th*** time step, $V_D(t_i)$ is the total flammable volume exposed at the ***i-th*** time step and $F_C(t_i)$ and $F_D(t_i)$ are the fractions of continuous and discrete ignition sources active in the area, respectively. λ_C and λ_D are evaluated by adding the contribution of each piece of equipment depending on its category (see Table 2 and Table 3 (Cincotta et al., 2021)). The fraction of continuous and discrete ignition sources, $F_C(t_i)$ and $F_D(t_i)$, respectively, active at the considered ***i-th*** time step depends on the safety barriers of Isolation & Depressurization (I&D) set up for deactivating and isolating ignition sources in the presence of a detected flammable leakage.

Table 2. Parameters for continuous delayed IP evaluation.

Equipment category	λ_C
Rotating machinery	3.70e-6 $\left[\frac{1}{m^3}\right]$
Rotating machinery (per item exposed)	3.70e-3 $\left[\frac{1}{\text{item}}\right]$
Electrical equipment	1.80e-6 $\left[\frac{1}{m^3}\right]$
Other	6.00e-7 $\left[\frac{1}{m^3}\right]$

Table 3. Parameters for discrete delayed IP evaluation.

Equipment category	λ_D
Rotating machinery	1.50e-9 $\left[\frac{1}{m^3 s}\right]$
Rotating machinery (per item exposed)	3.70e-6 $\left[\frac{1}{\text{item}\cdot s}\right]$
Electrical equipment	1.50e-9 $\left[\frac{1}{m^3 s}\right]$
Other	1.20e-8 $\left[\frac{1}{m^3 s}\right]$

2.3. Total Ignition probability

At each time step t_i, the total IP $P_T(t_i)$ is calculated as:

$$P_T(t_i) = 1 - (1 - P_I(I)\chi_{0,i}) \cdot (1 - P_{C,i}(I)) \cdot (1 - P_{D,i}(I)) \tag{4}$$

where $\chi_{0,i}$ is:

$$\chi_{0,i} = \begin{cases} 1 & if\ i = 0 \\ 0 & if\ i > 0. \end{cases} \tag{5}$$

The total ignition probability $P_T(I)$ throughout the whole LOPC transient is, then, calculated as:

$$P_T(I) = \sum_{i}^{N} P_{T,i}(I). \tag{6}$$

To calculate the volumes $V_{new}(t_i)$ and $V_D(t_i)$, time-consuming CFD simulations are required (e.g., with the FLACS software (Sajid et al., 2021)), to provide the input to MISOF (Figure 2).

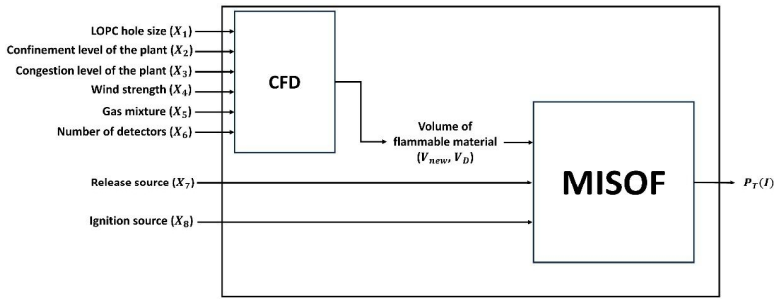

Fig. 2. $P_T(I)$ calculation sketch.

3. Regression model for IP estimation

3.1 Polynomial regression models

Given a dataset of N_d input patterns $\{\boldsymbol{X}, P_T(I)\}$, a linear regression model to estimate $P_T(I)$ can be written as:

$$\widehat{P_T}(I)(\boldsymbol{X}, w) = \sum_{j=0}^{M} w_j \varphi_j(\boldsymbol{X}), \tag{7}$$

where $\widehat{P_T}(I)(\boldsymbol{X}, w)$ is the estimated total IP and w_j are the coefficients of the basis functions $\varphi_j(\boldsymbol{X})$. In the case of polynomial regression, the basis functions take the form $\varphi_j(\boldsymbol{X}) = \boldsymbol{X}^j$. Piecewise polynomial basis functions can be defined to divide the input space into regions (Hastie et al., 2001). The defined basis functions are, then, fitted by minimizing the Mean Squared Error (MSE):

$$MSE = \frac{1}{N_d} \sum_{z=1}^{N_d} \left(P_{T,z}(I) - \widehat{P_{T,z}}(I)\right)^2 = \frac{1}{N_d} \sum_{z=1}^{N_d} e_z^2, \tag{8}$$

where e_z is the error of the output estimate $\widehat{P_{T,z}}(I)$ with respect to the target value $P_{T,z}(I)$ of the ***z-th*** pattern. Figure 3 shows the input and output of the polynomial regression model for IP estimation considered in this work.

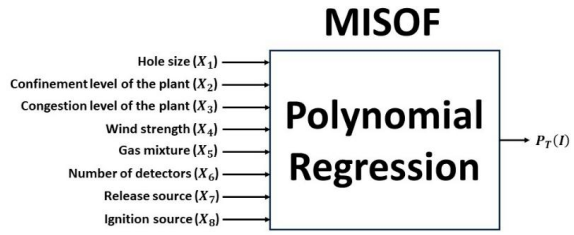

Fig. 3. Polynomial regression inputs and output.

3.2 Bayesian Regularized Artificial Neural Networks

BRANNs have been introduced to limit the problem of overfitting of traditional ANNs (Shi et al., 2018). Instead of minimizing only the MSE between the output estimates and the target values, BRANNs minimize the weighted sum of the MSE and of a second term (E_w) that accounts for the uncertainty in the model weights (Bishop, 2006):

$$F(w) = \beta MSE + \alpha E_w, \tag{9}$$

$$E_w = \frac{1}{m} \sum_{j=1}^{m} w_j^2, \tag{10}$$

where $F(w)$ is the objective function, α and β are hyper-parameters to be tuned, m is the number of weights and N is the number of input-output patterns.

Furthermore, Bayesian inference is used to update the density function of the weight vector $\boldsymbol{w}$:

$$P(\boldsymbol{w}|D, \beta, \alpha) = \frac{P(D|\boldsymbol{w}, \beta) \cdot P(\boldsymbol{w}|\alpha)}{P(D|, \beta, \alpha)} \tag{11}$$

where Gaussian approximations are used for the conditional probability distributions $P(D|\boldsymbol{w}, \beta)$ and $P(\boldsymbol{w}|\alpha)$. Then, the optimal weights are found by maximizing (11) (which corresponds to minimizing (9)), and the optimal values of α and β are calculated with the following equations:

$$\alpha = \frac{\gamma}{2E_w}, \tag{12}$$

$$\beta = \frac{N - \gamma}{2MSE}, \tag{13}$$

where γ is a measure of the number of parameters effectively used by the BRANN (i.e., the model weights that are not set to zero by the regularization process) to avoid overfitting and is found with an iterative procedure since it depends on α.

4. The novel BRANN

In (Di Maio et al., 2021a), a BRANN has been developed for IP estimation. This BRANN is capable of providing accurate IP estimates only when fed with input values similar to those of its training dataset. To extend the applicability of the BRANN metamodel to accidental scenarios with different LOPC hole sizes, the following strategy (shown in Figure 4) has been developed. For each functional unit and for each possible LOPC hole size X_1^{FU}:

- a suitable simulation software (e.g., Phast (Chen, 2020)) is run to calculate the peak gas leak flow rate Q_0^{FU} (i.e., the leak flow rate at $t = 0$) resulting from a LOPC in the selected functional unit with the due hole size;
- Q_0^{FU} is compared with the peak gas leak flow rate Q_0^T resulting from the hole sizes (X_1) used to train the BRANN;
- a conservative (i.e., with a larger leak flow rate) equivalent hole size (X_1^{EQ}) is calculated and fed to the BRANN, by selecting the smallest X_1 generating $Q_0^T \geq Q_0^{FU}$.

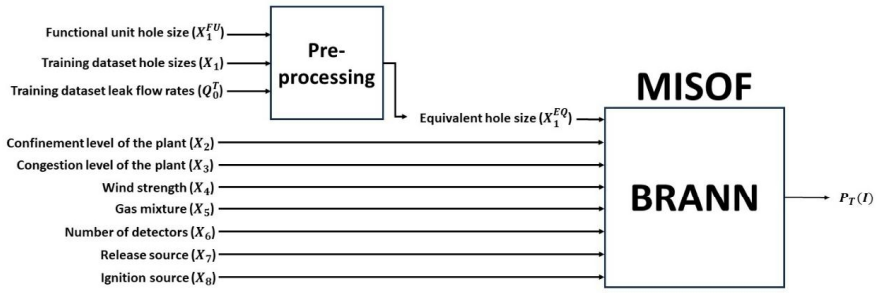

Fig. 4. Novel MISOF calculation approach.

5. Case study

As an example of application, let us consider a typical O&G plant, where the following functional units are installed:

1. *Inlet manifold*, with oil and gas as working fluids;
2. *Test separator A*, with oil and gas as working fluids;
3. *Test separator B*, with oil and gas as working fluids;
4. *Test separator C*, with oil and gas as working fluids;
5. *Separator 1*, with oil and gas as working fluids;
6. *Separator 2*, with oil and gas as working fluids;
7. *KO drum torch*, with oil and gas as working fluids;
8. *Gas boat*, with oil as working fluid;
9. *Booster pump*, area manifold with oil as working fluid;
10. *Gun barrel*, with oil as working fluid;
11. *Fluxing manifold*, with oil as working fluid;
12. *Gas network*, with gas as working fluid;
13. *Steam production boiler*, with gas as working fluid.

LOPC is considered to occur in the separator functional unit "Test separator A", with hole sizes X_1^{FU} of $7\ mm$, $22\ mm$, $70\ mm$ and $100\ m$, where only gas is the working fluid.

A state-of-practice variance-based sensitivity analysis (Saltelli et al., 2009) has been performed to reduce the number of inputs to the BRANN. As a result, the number of detectors (X_6) has been neglected because not contributing enough to the variance of $P_T(I)$, as shown in Table 4, where the η^2 of the $X_1, \dots, X_6$ inputs are listed. It is important to note that the sensitivity analysis has not been performed for inputs X_7 and X_8 (release source and ignition source, respectively), since they cannot be removed from the analysis.

Table 4. Sensitivity analysis results (η^2).

BRANN input	η^2
X_1	0.9180
X_2	0.0090
X_3	0.0092
X_4	0.0620
X_5	0.0014
X_6	0.00036

A BRANN has, then, been trained, composed of an input layer, three hidden layers (with 80, 60 and 40 neurons) and an output layer with 1 neuron. Table 5 reports the four types of confinement schemes, six levels of environmental congestion, two atmospheric conditions, three flammable cloud compositions, four LOPC hole sizes originated from three possible types of release sources in presence of four different types of ignition sources considered. This amounts to 20376 working configurations and hazardous conditions to be considered. Among these, only 14263 random configurations have been simulated by CFD, constituting an enough dense training dataset (as shown in (Di Maio et al., 2021a)).

Table 5. BRANN input variables.

Input variable	Input name	Values
X_1	LOPC hole size	$5\ mm$ $20\ mm$ $50\ mm$ $100\ mm$
X_2	Confinement level of the plant	"A" "B" "C" "D"
X_3	Congestion level of the plant	0 0.3 0.7 1 1.3 1.7
X_4	Wind strength	"5D" "2F"
X_5	Gas mixture	"Light" "Neutral" "Heavy"
X_7	Release source	"Pump" "General" "Other"
X_8	Ignition source	"Electrical machinery" "Rotating machinery" "All" "Other"

To use the trained BRANN for LOPC hole sizes of the separator different from those of the training dataset, the preprocessing described in Section 4 has been applied. In particular, Q_0^{FU} has been calculated with a commercial tool for each X_1^{FU}, to be compared with Q_0^T that are the peak leak flow rates of the hole sizes used for the training of the BRANN, that result from facilities and equipment different from those here considered. The procedure to find the conservative hole sizes is sketched in Figure 6. For example, for $X_1^{FU} = 7\ mm$ and $X_1^{FU} = 22\ mm$, the equivalent hole size is conservatively taken equal to $X_1^{EQ} = 5\ mm$ (assuming that, in both cases Q_0 is equal to $0.4240 \frac{kg}{s}$, that is the one that FLACS takes for $X_1 = 5\ mm$), and for $X_1^{FU} = 70\ mm$ and $X_1^{FU} = 100\ mm$ the equivalent hole size is conservatively taken equal to $X_1^{EQ} = 20\ mm$ (assuming that, in both

cases Q_0 is equal to $6.7695\frac{kg}{s}$, that is the one that FLACS takes for $X_1 = 20\,mm$), as also summarized in Table 6.

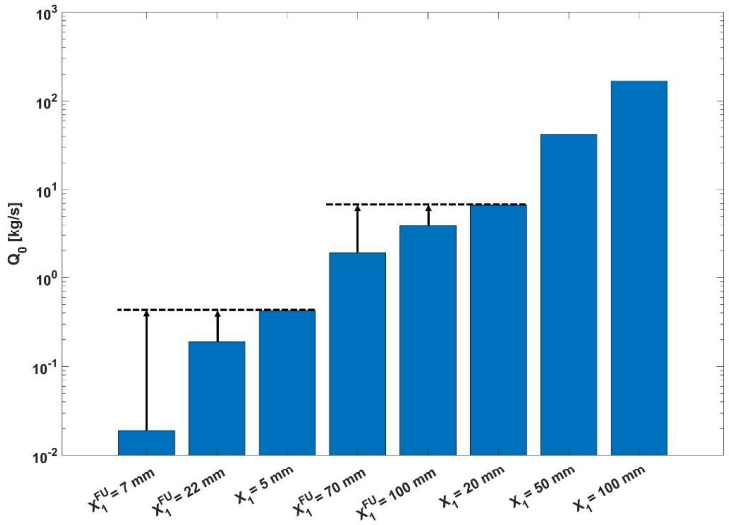

Fig. 6. Leak flow rate comparison.

Table 6. LOPC hole sizes equivalence.

X_1^{FU}	X_1^{EQ}
7 mm	5 mm
22 mm	5 mm
70 mm	20 mm
100 mm	20 mm

The novel approach is tested on the four input batches (S_s with $s = 1,2,3,4$) listed in Table 7, representative of typical configurations of hole sizes, confinement levels, congestion levels, wind strengths, gas mixtures, release sources and ignition sources that might occur in the neighborhood of "Test separator A", and the IP estimates obtained are compared to those provided by a polynomial regression fitted on the same dataset and with the true value retrieved from the full dataset of FLACS simulations (Figure 7). The BRANN provides IP estimates for all four batches of input with much larger accuracy ($MSE_{BRANN} = 9.99 \cdot 10^{-10}$) than the polynomial regression ($MSE_{poly} = 3.13 \cdot 10^{-5}$), that incidentally also overestimates the true IP.

Table 7. BRANN input sequences for "Test separator A".

	X_1^{EQ}	X_2	X_3	X_4	X_5	X_7	X_8
S_1	5 mm	A	0.7	2F	Light	General	All
S_2	5 mm	A	0.7	5D	Light	General	All
S_3	20 mm	A	0.7	2F	Light	General	All
S_4	20 mm	A	0.7	5D	Light	General	All

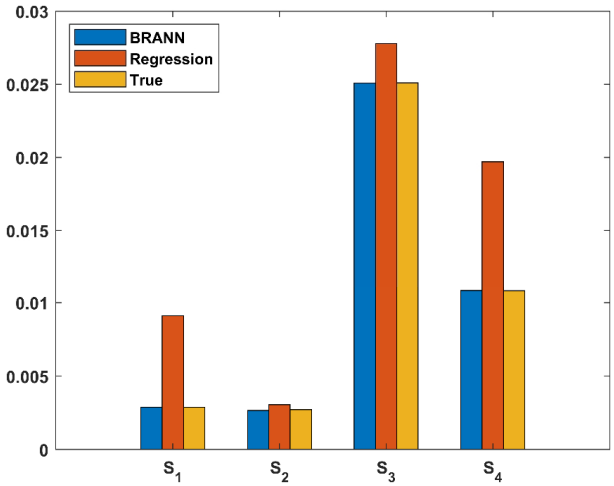

Fig. 7. IP estimates comparison.

The practical applicability of the BRANN for in field risk assessment is shown by the savings of computational time: for each input combination $(X_1, \dots, X_8)$ the IP estimation with the MISOF model and CFD simulations requires several hours, while the BRANN only takes 0.01 seconds on a commercially available laptop equipped with an AMD Ryzen 5 PRO 4650U processor.

6. Conclusions

For QRA of O&G plants, IP can be estimated with the MISOF model, which requires time-consuming CFD simulations to calculate the flammable volume released. To address this issue, this work builds upon a previous approach based on a BRANN to further extend its applicability by proper preprocessing of the input LOPC hole size. The results obtained on a real case study show that the preprocessing strategy extends applicability to LOPC hole sizes of values different from those of the training dataset. The developed method will find practical application through the development of an operational risk assessment tool (for example, being embedded into (Di Maio et al., 2021b)) for assessing the risk associated with fires and explosions in O&G facilities.

References

Agranat, V., Tchouvelev, A. V., Cheng, Z., Zhubrin, S. V. 2007. CFD Modeling of Gas Release and Dispersion: Prediction of Flammable Gas Clouds. In Advanced Combustion and Aerothermal Technologies, 179–195. Springer Netherlands. https://doi.org/10.1007/978-1-4020-6515-6_14

Bishop, C. M. 2006. Pattern Recognition and Machine Learning. Springer New York, NY.

Chen, Y. 2020. Consequence Simulation and Risk Assessment Model of Liquid Ammonia Leakage Accident Based on PHAST Software. 2020 International Conference on Advance in Ambient Computing and Intelligence (ICAACI), 125–129. https://doi.org/10.1109/ICAACI50733.2020.00032

Cincotta S., Crivellari A., La Rosa L., Decarli L. 2021. MISOF Model: A novel approach for ignition probability estimation in offshore installations. 15th OMC Med Energy Conference and Exhibition.

Di Maio, F., Scapinello, O., Zio, E., Cincotta, S., Crivellari, A., Decarli, L., Rosa, L. 2021a. A Bayesian Regularized Artificial Neural Network for the Estimation of the Ignition Probability in Accidents in Oil & Gas Plants, 2310–2314. https://doi.org/10.3850/978-981-18-2016-8_703-cd

Di Maio, F., Scapinello, O. Zio, E., Ciarapica, C., Cincotta, S., Crivellari, A., Decarli, L., Rosa, L. 2021b. Accounting for Safety Barriers Degradation in the Risk Assessment of Oil and Gas Systems by Multistate Bayesian Networks. Reliability Engineering and System Safety. https://doi.org/10.1016/j.ress.2021.107943

Hastie, T., Tibshirani, R., Friedman, J. 2001. The Elements of Statistical Learning. Springer.

IOGP 434-06. 2019. Ignition probability, International Association of Oil & Gas Producers.

ISO 17776. 2016. Petroleum and natural gas industries - Offshore production installations – Major accident hazard management during the design of new installations.

Jin, Y. L., Jang, B. S. 2018. Probabilistic explosion risk analysis for offshore topside process area. Part I: A new type of gas cloud frequency distribution for time-varying leak rates. Journal of Loss Prevention in the Process Industries 51, 125–136. https://doi.org/10.1016/j.jlp.2017.12.008

MISOF. 2018. Modelling of ignition sources on offshore oil and gas facilities – MISOF, Report for Norwegian Oil and Gas Association, Report no: 107566/R2. https://offshorenorge.no/contentassets/067198d80b9c4b039b879bd0c8ae42bf/107566_r2_final_.pdf

Sajid, Z., Khan, M. K., Rahnama, A., Moghaddam, F. S., Vardhan, K., Kalani, R. 2021. Computational fluid dynamics (Cfd) modeling and analysis of hydrocarbon vapor cloud explosions (vces) in amuay refinery and jaipur plant using flacs. Processes 9(6). https://doi.org/10.3390/pr9060960

Saltelli, A., Chan, K., Scott, E. M. 2009. Sensitivity Analysis. Wiley.

Shi, J., Khan, F., Zhu, Y., Li, J., Chen, G. 2018. Robust data-driven model to study dispersion of vapor cloud in offshore facility. Ocean Engineering 161, 98–110. https://doi.org/10.1016/J.OCEANENG.2018.04.098

Vianna, S. S. V., Cant, R. S. 2012. Explosion pressure prediction via polynomial mathematical correlation based on advanced CFD Modelling. Journal of Loss Prevention in the Process Industries 25(1), 81–89. https://doi.org/10.1016/j.jlp.2011.07.005

Zhang, B., Chen, G. M. 2010. Quantitative risk analysis of toxic gas release caused poisoning - A CFD and dose-response model combined approach. Process Safety and Environmental Protection 88(4), 253–262. https://doi.org/10.1016/j.psep.2010.03.003